

**Supporting Information: Ultra-Sensitive Potentiometric Measurements of Dilute Redox Molecule
Solutions and Determination of Sensitivity Factors at Platinum Ultramicroelectrodes**

Stephen J. Percival and Allen J. Bard*

Center for Electrochemistry, Department of Chemistry, The University of Texas at Austin, Austin Texas 78712, USA

* Corresponding author, Phone: (512) 471-3761, email: ajbard@mail.utexas.edu

Table of Contents:

Chemicals and Materials.....	S-2
Further Discussion.....	S-3
Figure S-1: Mass Transfer Limited Current CVs of Pt UMEs.....	S-5
Figure S-2: Example Potential vs Time Curve.....	S-6
Figure S-3: OCP Experimental and Calculation Curve Comparison 1.9 μm Radius Pt.....	S-7
Figure S-4: OCP Curves for 48 nm Radius Pt UME.....	S-8
Figure S-5: OCP Comparison Curves for 1-Propanethiol Modified Pt.....	S-9
References.....	S-10

Chemicals and Materials

All aqueous solutions were prepared using deionized water (>18 MΩ cm, Milli-Q) and all chemicals and materials were used as received from the manufacturers. Potassium chloride (KCl, Fisher Scientific), monobasic potassium phosphate (KH₂PO₄, J. T. Baker), dibasic potassium phosphate (K₂HPO₄, J. T. Baker), potassium hydroxide (KOH, Fisher Scientific), Hydrochloric acid (HCl, concentrated Fisher Scientific), Potassium Ferricyanide (K₃Fe(CN)₆, Fisher Scientific), Potassium Ferrocyanide tri-hydrate (K₄Fe(CN)₆ · 3H₂O, Fisher Scientific), Ethanol (200 proof, Pharmco-Aaper), 1-propanethiol (99%, Sigma-Aldrich), Argon (99.9%, Praxair) were used without further purification.

Further Discussion

Redox concentrations (equimolar K₃Fe(CN)₆ and K₄Fe(CN)₆) used in the OCP plot of Figure 3A of the main text include pure electrolyte (no redox molecules), 5 nM, 50 nM, 500 nM, 1 μM, 3 μM, 5 μM, 10 μM, 25 μM, 50 μM, 100 μM, 300 μM, 500 μM and 5 mM. For the OCP plot of Figure 3B of the main text include pure electrolyte (no redox molecules), 5 nM, 50 nM, 500 nM, 1 μM, 3 μM, 5 μM, 50 μM, 500 μM and 5 mM. These represent typical values of the redox concentrations used for many of the rest of the OCP measurement experiments.

These experiments were performed using platinum UMEs of various sizes. The ferrocene methanol (FcMeOH) CVs used to confirm the sizes of the smaller UMEs from their mass transport limited currents are shown in Figure S1. The CVs reach a plateau which is the diffusion limited current, where no additional current can be attained from the oxidation of the redox molecule. Using this limiting value the size of the UME can be calculated from equation 1 below, which is for a planar disk electrode.¹

$$i_{DL} = 4nFDCr \quad (1)$$

Where n is the number of electrons transferred per redox molecule, F is Faraday constant, D is the diffusion coefficient of the redox molecule (for FcMeOH D = 6.7x10⁻⁶ cm²/s),² C is the bulk

concentration of the redox molecule and r is the radius of the electrode. The mass transfer limited currents observed for the two electrodes seen in Figure S-1 are approximately 977 pA and 25 pA. From these limited currents observed for the two small UMEs we have determined from equation 1 that the electrode sizes were $\sim 1.9 \mu\text{m}$ radius and $\sim 48 \text{ nm}$ radius.

Figure S-2 shows a typical potential vs time curve from a $12.5 \mu\text{m}$ radius Pt electrode in 100 mM phosphate buffer (pH 7.4). The measured potential curve is seen to start at a more positive potential than the final equilibrium potential and quickly decreases. As the potential decreases towards the equilibrium potential the rate of change slows and is seen to follow an exponential decay curve. The shape of this example curve is very similar to other potential vs time curves obtained in other tested electrolytes, such as KCl and KOH. The difference in other electrolytes being the equilibrium OCP which is determined to be pH dependent. We typically defined the steady state OCP as where the OCP would change by less than 1 mV/min. This was done in an attempt to reduce possible reference electrode drift and solution changes over the course of a long experiment.

Figure S-3 shows the comparison of the experimental and calculated OCP curves as a function of the redox concentration obtained from the $1.9 \mu\text{m}$ radius Pt electrode in de-aerated 100 mM KCl shown in Figure 3C of the main text. The calculated values for the OCP at each concentration were obtained using most of the same parameters listed in Table 1 of the main text, but with some slightly changed with values listed in the figure caption. The resulting calculated plot follows very closely to the experimental plot again demonstrating the effectiveness of calculating the half reactions that make up the observed mixed potential. From the calculated curve the partial currents for each half reaction could be determined and used to derive the sensitivity factors for the electrode, which is shown in Figure 7 of the main text.

A much smaller electrode (48 nm radius Pt UME) was used to observe the OCP at dilute concentrations of redox molecules in the same manner as was done with the larger electrode. It was thought that the smaller sized electrode would show a change in the OCP at much more dilute concentrations. Figure S-4 shows the results from the 48 nm radius electrode in 100 mM KCl that has

been de-aerated (Figure S-4A) and that is air saturated (Figure S-4B). Figure S-4A shows that there is essentially no change in the OCP at pico- and nano-molar levels and again does not change until micro-molar levels are reached, similar to the larger electrodes. The corresponding calculated OCP curve, that is seen to match the experimental data well, was made with many parameters listed in Table 1 of the main text but some slightly changed and are listed in the figure caption. The air saturated OCP curve again shows very similar behavior as observed for the larger 1.9 μm radius electrode. The mixed potential starts at a more positive value than the redox formal potential and is seen to shift negatively as the redox concentration is increased.

Figure S5A shows the comparison of the experimental and calculated OCP curves for a 1-propanethiol modified 12.5 μm radius platinum electrode in de-aerated 100 mM phosphate buffer (pH 7.4). Again the calculated curve was made using many parameters from Table 1 in the main text but with some changed parameters that are listed in the figure caption. The curve fits the experimental data very well and it is worth noting that the rate constants are drastically smaller than what is used for the bare electrode. This is attributed to the propanethiol layer hindering the inner-sphere reactions. Figure S-5B shows the un-normalized OCP data comparing a propanethiol modified Pt electrode and a bare Pt electrode. This data is shown as a normalized plot in Figure 6D of the main text. The modified electrode OCP begins at a much more positive potential as compared to the bare electrode because the surface layer is blocking the inner-sphere reactions (mainly water oxidation). It is also seen to respond shift the OCP at lower concentrations and finally become *poised* before the bare Pt electrode does.

Figure S-1: CVs from (A) the $\sim 1.9 \mu\text{m}$ radius Pt UME and (B) the $\sim 48 \text{ nm}$ radius Pt UME in 2 mM FcMeOH and 100 mM KCl. Scan rate was 50 mV/s and solutions were de-aerated with Ar.

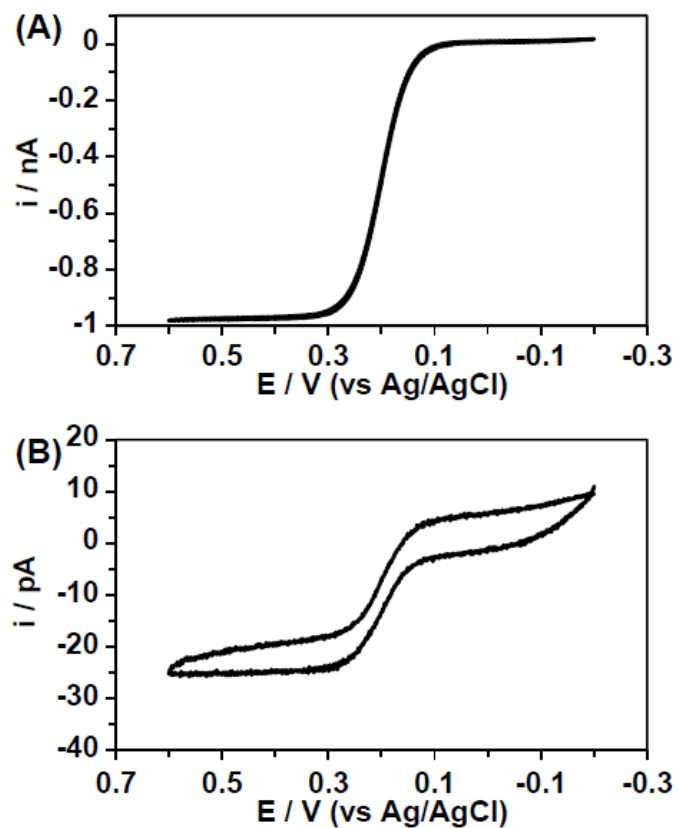


Figure S-2: A typical potential vs time potential curve from a 12.5 μm radius Pt UME in 100 mM phosphate buffer (pH 7.4) with Ar bubbling through the solution for the duration of the trace.

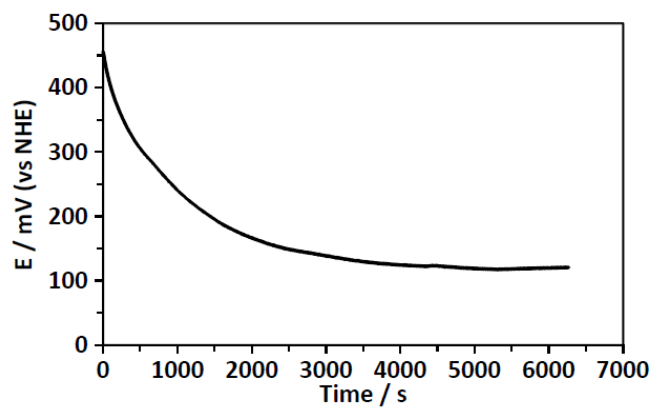


Figure S-3: OCP vs $-\log$ plot of the redox concentration for the 1.9 μm radius Pt electrode in de-aerated 100 mM KCl along with the calculated OCP curve. Calculated curve made using the same constants listed in the main text with a measured pH of 6.7 (due to an unbuffered solution) and $k_{\text{C}1}^{\circ}(\text{O}_2) = 0.005 \text{ cm/s}$, $k_{\text{A}2}^{\circ}(\text{H}_2\text{O}) = 4.2 \times 10^{-6} \text{ cm/s}$, $C_{\text{O}_2}^* = 1 \times 10^{-6} \text{ mol/L}$, $k_{\text{C}3}^{\circ} = k_{\text{A}4}^{\circ} = 0.01 \text{ cm/s}$.

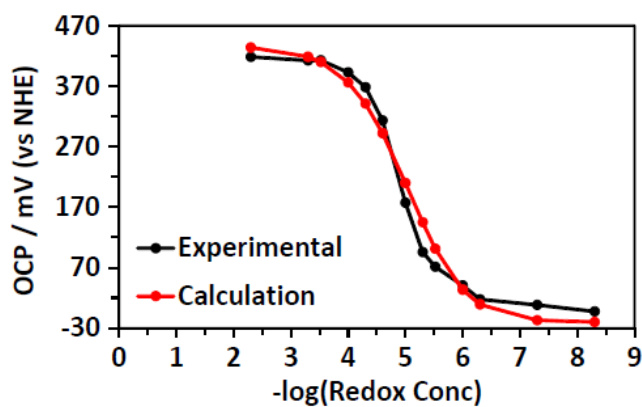


Figure S-4: OCP vs $-\log$ redox concentration curves obtained from a 48 nm radius Pt electrode. (A) Ar bubbled 100 mM KCl with corresponding calculated OCP curve and (B) air saturated 100 mM KCl. Calculated curve in (A) made using the same constants listed in the main text with a measured pH of 6.7 (due to an unbuffered solution) and $k_{C1}^o(O_2) = 0.05$ cm/s, $k_{A2}^o(H_2O) = 1.5 \times 10^{-5}$ cm/s, $C_{O_2}^* = 5 \times 10^{-6}$ mol/L, $\alpha_{C1}(O_2) = 0.5$, $\alpha_{A2}(H_2O) = 0.82$, $k_{C3}^o = k_{A4}^o = 0.05$ cm/s.

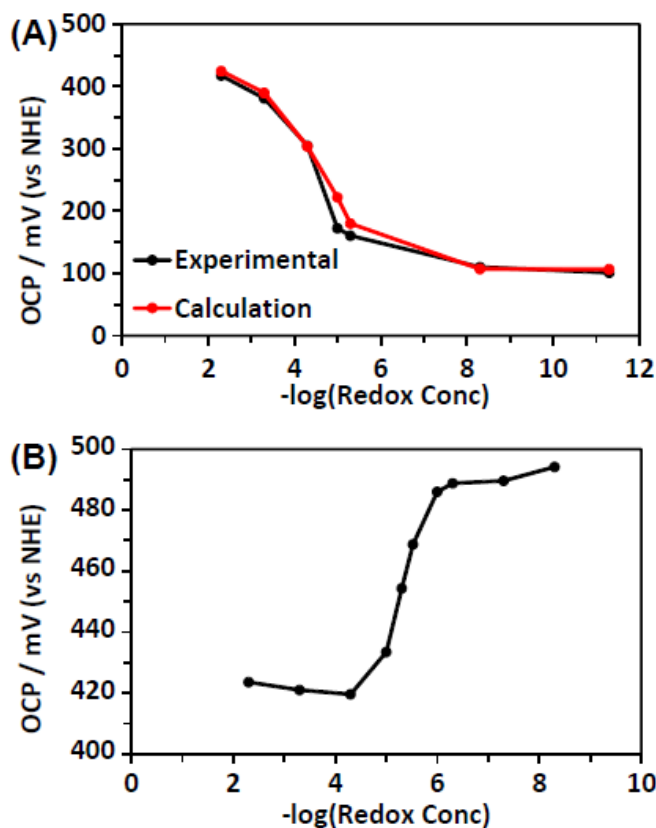
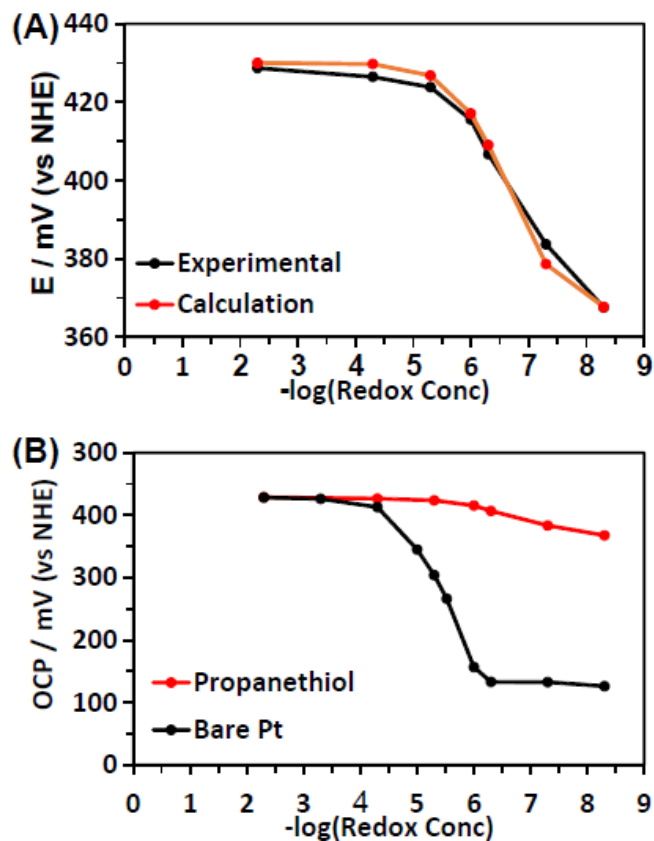


Figure S-5: (A) Comparison of the experimental and calculated OCP curves for the 1-propanethiol modified electrode. (B) Un-normalized comparison of the OCP change with concentration between a 1-propanethiol modified Pt electrode and a bare Pt electrode. Solutions were de-aerated 100 mM PB (pH 7.4). Calculated curve in (A) made using the same constants listed in the main text and $k_{C1}^0(O_2) = 8 \times 10^{-6}$ cm/s, $k_{A2}^0(H_2O) = 9.4 \times 10^{-12}$ cm/s, $\alpha_{A2}(H_2O) = 0.7$, $k_{C3}^0 = k_{A4}^0 = 9 \times 10^{-6}$ cm/s.



Additional References

- (1) Bard, A. J.; Faulkner, L. R. *Electrochemical Methods*. 2nd ed.; John Wiley & Sons: New York, 2001.
- (2) Anicet, N.; Bourdillon, C.; Demaille, C.; Moiroux, J.; Savéant, J.-M. *J. Electroanal. Chem.* **1996**, *410*, 199–202.